The AAPS Journal, Vol. 18, No. 1, January 2016 (© 2015)
DOI: 10.1208/s12248-015-9827-4

Research Article

Gomisin A is a Novel Isoform-Specific Probe for the Selective Sensing of Human Cytochrome P450 3A4 in Liver Microsomes and Living Cells

Jing-Jing Wu,[1,2] Guang-Bo Ge,[1] Yu-Qi He,[1] Ping Wang,[1] Zi-Ru Dai,[1,2] Jing Ning,[1] Liang-Hai Hu,[3] and Ling Yang[1,4]

Received 25 June 2015; accepted 31 August 2015; published online 11 September 2015

Abstract. Nearly half of prescription medicines are metabolized by human cytochrome P450 (CYP) 3A. CYP3A4 and 3A5 are two major isoforms of human CYP3A and share most of the substrate spectrum. A very limited previous study distinguished the activity of CYP3A4 and CYP3A5, identifying the challenge in predicting CYP3A-mediated drug clearance and drug–drug interaction. In the present study, we introduced gomisin A (GA) with a dibenzocyclooctadiene skeleton as a novel selective probe of CYP3A4. The major metabolite of GA was fully characterized as 8-hydroxylated GA by LC-MS and NMR. CYP3A4 was assigned as the predominant isozyme involved in GA 8-hydroxylation by reaction phenotyping assays, chemical inhibition assays, and correlation studies. GA 8-hydroxylation in both recombinant human CYP3A4 and human liver microsomes followed classic Michaelis-Menten kinetics. The intrinsic clearance values indicated that CYP3A4 contributed 12.8-fold more than CYP3A5 to GA 8-hydroxylation. Molecular docking studies indicated different hydrogen bonds and π–π interactions between CYP3A4 and CYP3A5, which might result in the different catalytic activity for GA 8-hydroxylation. Furthermore, GA exhibited a stronger inhibitory activity towards CYP3A4 than CYP3A5, which further suggested a preferred selectivity of CYP3A4 for the transformation of GA. More importantly, GA has been successfully applied to selectively monitor the modulation of CYP3A4 activities by the inducer rifampin in hepG2 cells, which is consistent with the level change of CYP3A4 mRNA expression. In summary, our results suggested that GA could be used as a novel probe for the selective sensing of CYP3A4 in tissue and cell preparations.

KEY WORDS: CYP3A4; gene induction; Gomisin A; isoform-specific probe; selective sensing.

INTRODUCTION

Cytochromes P450 (CYP) 3A4 and CYP3A5 are responsible for the metabolism of more than 50% of drugs currently on the market [1]. CYP3A4 is the predominant P450 form expressed in the human liver and intestine. In contrast, CYP3A5 is expressed polymorphically [2], which might contribute as much as 50% of hepatic P450 3A in one third of all Caucasians and one half of all African-Americans [3]. Although CYP3A4 and CYP3A5 share an 83% amino acid sequence identity and have overlapping substrate specificities [4], the two isoforms behave differently with respect to their catalytic activity and inhibition potency. For example, the activity of CYP3A4 is generally higher than that of CYP3A5. However, CYP3A5 was more active than CYP3A4 in catalyzing total midazolam hydroxylation and exhibited comparable metabolic activity as CYP3A4 toward dextromethorphan N-demethylation and carbamazepine epoxidation [5]. Erythromycin and verapamil inactivate CYP3A5 at a slower rate than their respective effects on CYP3A4 [6, 7]. Therefore, defining their respective contributions to drug metabolism as well as drug–drug interactions (DDIs) in the process of drug discovery and clinical drug therapy remains challenging.

Electronic supplementary material The online version of this article (doi:10.1208/s12248-015-9827-4) contains supplementary material, which is available to authorized users.

[1] Laboratory of Pharmaceutical Resource Discovery, Dalian Institute of Chemical Physics, Chinese Academy of Sciences, 457 Zhongshan Road, Dalian, 116023, China.
[2] Graduate University of Chinese Academy of Sciences, 19A Yuquanlu, Beijing, 100049, China.
[3] Research Center for Drug Metabolism, College of Life Science, Jilin University, Changchun, 130012, China.
[4] To whom correspondence should be addressed. (e-mail: yling@dicp.ac.cn)

ABBREVIATIONS: 8-HGA, 8-Hydroxy-gomisin A; ABT, 1-Aminobenzotriazole; CCK-8, Cell counting kit-8; CL_{int}, Intrinsic clearance; CYP, Cytochrome P450; DGA, Demethylene-gomisin A; DMEM, Dulbecco's modified Eagle's medium; ESI, Electrospray ionization; FCS, Fetal calf serum; GA, Gomisin A; HLM, Human liver microsomes; IC_{50}, Half maximal inhibitory concentration of a substance; K_m, Apparent affinity; NADPH, Nicotinamide-adenine dinucleotide phosphate; rhCYP, Recombinant human cytochrome P450; thioTEPA, Triethylenethiophosphoramide; UFLC-DAD, Ultra-fast liquid chromatography-diode array detector; V_{max}, Apparent maximum reaction velocity; NMR, Nuclear magnetic resonance.

Variability in the CYP3A4 protein levels and enzyme activities resulting from its susceptibility to induction and inhibition greatly contributes to large interindividual variability in drug responses [8]. Consequently, evaluating the inhibitory and inductive potential of drug candidates toward CYP3A4 to estimate their potential DDI in the early stage of drug discovery is necessary [9]. However, because of the existence of several distinct binding sites in CYP3A4, a poor correlation of CYP3A4 activity represented by different CYP3A4 probes is frequently observed in the *in vitro* assessment [10]. Therefore, it is recommended that multiple CYP3A4 probes should be used for the quantification of CYP3A4 activity in enzyme systems (e.g., liver microsomes and cells).

In the last few decades, numerous efforts have been made to specifically detect the CYP3A4 activity in liver microsomes and living cells. A qualified CYP3A4 probe should: (1) have high selectivity, (2) have high sensitivity, (3) have high permeability and be non-toxic, (4) follow simple Michaelis-Menten kinetics, and (5) be commonly available. However, the application of the luminescence probe of CYP3A4 [11] is limited by its relatively high cost and high vulnerability to changes in ionic strength or pH according to the above requirements. Moreover, it is noteworthy that testosterone (a steroid compound), as the most commonly used CYP3A4 substrate, is metabolized by both CYP3A4 and CYP3A5 [12] and its metabolic behavior follows non-Michaelis-Menten kinetics [13]. Nevertheless, CYP3A4 and CYP3A5 display different catalytic preferences on the steroid compounds. Previously, we reported that bufalin was an excellent probe to selectively detect CYP3A4 activity in liver microsomes [14]. Bufalin is a natural bufodienolide with a rigid steroid skeleton that is a good substrate for CYP3A4 but a poor substrate of CYP3A5. This finding supports the fact that the active site cavity of CYP3A4 is larger than that of other CYPs [15, 16], resulting in the better adaptability of CYP3A4 to rigid molecules.

Recently, we also found that CYP3A played a key role in the biotransformation of natural lignans (such as schizandrin and deoxyschizandrin) with the dibenzocyclooctadiene skeleton from *Fructus Schisandrae Chinensis* [17, 18]. Notably, these naturally occurring lignans also have a rigid polycyclic skeleton, but they are non-steroidal compounds. In contrast to bufodienolides (such as bufalin), which are potent cytotoxic agents that strongly limit their application for selectively measuring CYP3A4 activity in living cells [19, 20], lignans are relatively non-toxic [21]. To find a probe with the expected features for the detection of CYP3A4 activity, we screened the structurally similar dibenzocyclooctadiene lignans (Supplemental Fig. S1). Our preliminary experiments indicated that the metabolic capability of gomisin A (GA) with CYP3A5 is very limited compared to CYP3A4. Therefore, we hypothesized that GA might be a novel isoform-specific probe of human CYP3A4 that meets the desired features.

The aim of the present study was, therefore, to find further support that GA may serve as a selective probe substrate for CYP3A4 and could probe the real functions of CYP3A4 in various biological samples, such as microsomes and living cells. Then, we preliminarily explored the enzyme structure-catalytic specificity relationships of CYP3A4 and CYP3A5 through molecular docking simulations.

MATERIALS AND METHODS

Chemicals and Reagents

Gomisin (GA) was purchased from Sichuan WeiKeqi Biological Technology Co., Ltd. (Chengdu, China). 1-Aminobenzotriazole (ABT), sulfaphenazole, quinidine, clomethiazole, furafylline, 8-methoxypsoralen, omeprazole, CYP3cide, nifedipine, midazolam, testosterone, glucose-6-phosphate dehydrogenase, $NADP^+$, D-glucose-6-phosphate, rifampin, and trypsin (TPCK-treated, from bovine pancreas) were purchased from Sigma (St. Louis, MO, USA). Ketoconazole was obtained from ICN Biomedicals, Inc. (Aurora, Ohio, USA). Montelukast was purchased from Beijing Aleznova Pharmaceutical (Beijing, China). Triethylenethiophosphoramide (thioTEPA) was purchased from Acros Organics (Geel, Belgium). Bufalin was purchased from Shanghai Boyle Chemical Company (Shanghai, China). Dulbecco's modified Eagle's medium (DMEM) and fetal calf serum (FCS) were purchased from Invitrogen. A cell counting kit-8 (CCK-8) was purchased from Solarbio (Beijing, China). All other reagents were of the highest commercially available grade.

Enzyme Source

cDNA-expressed recombinant human cytochrome P450 (rhCYP) isoforms (P450 concentration is 1 nmol/ml, total protein is 10 mg/ml), including CYP 1A1, CYP1A2, CYP1B1, CYP2A6, CYP2B6, CYP2C8, CYP2C9, CYP2C19, CYP2D6, CYP2E1, CYP3A4, CYP3A5, CYP4F2, and CYP4F3B, derived from baculovirus-infected insect cells co-expressing NADPH-CYP reductase and cytochrome b5, were purchased from Cypex (Dundee, UK). Mixed human liver microsomes that were prepared from male Caucasians (25 donors) were obtained from BD Biosciences (MA, USA). A panel of 13 HLMs from individuals (male Mongolia) was obtained from Research Institute for Liver Diseases (Shanghai) Co. LTD (China). All of the microsomal samples and recombinant human CYP isoforms were stored at −80°C until use.

Analytical Instruments and Conditions

The UFLC system was equipped with a CBM-20A communications bus module, a SIL-20ACHT autosampler, two LC-20 AD pumps, a DGU-20A3 vacuum degasser, a CTO-20 AC column oven, and a SPD-M 20A diode array detector (DAD). A Hypersil ODS (C18) analytical column (150 mm×2.1 mm, 3 μm, Thermo Scientific) with a Hypersil ODS (C18) guard column (150 nm×2.1 mm, 3 μm, Thermo Scientific) was used to separate GA and its metabolites. The mobile phase consisted of CH_3OH (A) and water (B) with the following gradient profile: 0–2 min, 50% B; 2–9 min, 50–15% B; 9–12 min, 15–5% B; and 12–16.5 min, balanced to 50% B. The flow rate was 0.4 ml/min, and the column temperature was kept at 40°C. GA and its metabolites were detected at 254 nm. The metabolite concentrations were estimated against a standard curve with a linear range of 0.05 to 30 μM of GA, with a correlation coefficient >0.999.

A Shimadzu LC-MS-2010EV (Kyoto, Japan) instrument with an electrospray ionization (ESI) interface was used for

the identification of GA and its metabolite. Mass detection was performed in both positive-ion mode (ESI^+) and negative ion mode (ESI^-) from *m*/*z* 200 to 500. The detector voltage was set at +1.75 and −1.55 kV for positive and negative ion detections, respectively. The curved desolvation line temperature (CDL) and the block heater temperature were both set at 250°C. Other mass spectrometry (MS) detection conditions were as follows: the interface voltage was 4 kV, CDL voltage was 40 V, nebulizing gas (N_2) flow was 1.5 l/min and drying gas pressure was 0.06 MPa. Data processing was performed using LC-MS Solution software, version 3.41.

Incubation Conditions

The incubation mixture, with a total volume of 200 μl, consisted of 100 mM potassium phosphate buffer (100 mM KH_2PO_4/K_2HPO_4, pH 7.4), a NADPH-generating system (1 mM $NADP^+$, 10 mM glucose-6-phosphate, 1 unit/ml of glucose-6-phosphate dehydrogenase, and 4 mM $MgCl_2$), and human liver microsomes or CYPs with the designed concentration. In all of the experiments, GA (20 mM dissolved in methanol previously) was serially diluted to the required concentrations and the final concentration of methanol did not exceed 1% (*v*/*v*) in the mixture [22]. After preincubation at 37°C for 3 min, the reaction was initiated by adding an NADPH-generating system; the reaction was incubated at 37°C in a shaking water bath. The reaction was terminated by the addition of 200 μl of ice-cold methanol after the required incubation time. The mixture was kept on ice until it was centrifuged at 20,000×*g* for 20 min at 4°C. Aliquots of supernatants were stored at −20°C for less than 24 h until analysis. The stability of GA and its metabolite at 37°C for 24 h and at −20°C for 1 week has been previously tested, respectively, and no degradations of both GA and its metabolite were detected. Control incubations without an NADPH-generating system, without a substrate or without CYP enzyme sources, were carried out to ensure that metabolite formation was CYP- and NADPH-dependent. All of the incubations throughout the study were carried out in three experiments performed in duplicate with standard deviation (S.D.) values generally below 10%, and the results were expressed as the mean±S.D.

Reaction Phenotyping Assays with Recombinant P450s

Fourteen cDNA-expressed rhCYP isoforms co-expressing NADPH-P450 reductase (CYP1A1, CYP1A2, CYP1B1, CYP2A6, CYP2B6, CYP2C8, CYP2C9, CYP2C19, CYP2D6, CYP2E1, CYP3A4, CYP3A5, CYP4F2, and CYP4F3B) were used to screen the involved isoform(s) for the hydroxylation of GA in HLM. The incubations were carried out under the abovementioned incubation conditions with each CYP isoform. In reaction phenotyping assays, a relatively high substrate concentration (50 μM) was used and incubated with each recombinant human CYP (50 nM) at 37°C for 30 min. The reaction mixtures were centrifuged to precipitate the protein as described previously. The supernatants were then analyzed by UFLC-DAD to quantify the metabolites of GA.

Chemical Inhibition Assays

Chemical inhibition studies were performed by adding specific inhibitors for different CYP isoforms to the incubation mixture of GA to verify the involved enzyme(s). In brief, GA (10 μM, near K_m value) was incubated in mixed HLM (0.2 mg protein/ml) for 20 min with an NADPH-generating system in the absence (control) or presence of known CYP isoform-specific inhibitors. The inhibitors and their concentrations were as follows [23]: sulfaphenazole (10 μM) for CYP2C9, omeprazole (20 μM) for CYP2C19, quinidine (10 μM) for CYP2D6, clomethiazole (50 μM) for CYP2E1, ketoconazole (1 μM) for CYP3A, and montelukast (2 μM) for CYP2C8 [24]. Inhibition by the mechanism-based inhibitors: furafylline (10 μM) for CYP1A2, 8-methoxypsoralen (2.5 μM) for CYP2A6, TEPA (50 μM) for CYP2B6 [25], ABT (500 μM) for broad CYPs [26], and CYP3cide (1 μM) for CYP3A4 [27], were assayed by pre-incubation with an NADPH-generating system at 37°C for 20–30 min.

Correlation Studies

The formation rates of the metabolites described for GA (10 μM, near K_m value) were determined in a panel of HLMs prepared from 13 individual donors after 20 min incubation with an NADPH-generating system described as mentioned previously. These values were compared with the levels of CYP3A4 or CYP3A5 in 13 individual HLMs. Briefly, microsomes were digested by trypsin at 37°C for 14 h using an enzyme-to-substrate ratio of 1:50 as previously described [28]. Then, the digested sample was centrifuged for 10 min at 13,000*g*, and the supernatant was spiked with the stable isotope-labeled peptides of EVTNFLR (for CYP3A4) and SLGPVGFMK (for CYP3A5) as internal standards for LC-MS/MS analysis using the multiple reaction monitoring (MRM) mode. Specific peptides of EVTNFLR (for CYP3A4) and SLGPVGFMK (for CYP3A5) were selected for their quantification by using transition ions with ratios of 439.7/549.3 and 468.3/678.5, respectively. In addition, the 8-HGA formation rates were also compared with the activities of CYP3A4 and CYP3A5 by employing bufalin 5β-hydroxylation [14] and midazolam 1′-hydroxylation [5, 29] as the selective probe reactions at concentrations equal to their respective K_m values in 13 individual HLMs. The correlation parameter was expressed by the linear regression coefficient (*r*). $P<0.05$ was considered statistically significant.

Kinetics Analysis

To estimate the kinetic parameters of GA 8-hydroxylation in different enzyme sources, the incubation conditions were optimized to ensure that the formation rates of 8-HGA were in the linear range in relation to the incubation time and protein concentration at 37°C. GA (previously dissolved in methanol) was serially diluted to the required concentrations (1, 5, 10, 20, 50, 100, 200, and 300 μM), and the final concentration of methanol was 1% (*v*/*v*). GA was respectively incubated with mixed HLM (0.2 mg protein/ml), rhCYP3A4 and rhCYP3A5 (20 nM) for 20 min. All of the incubations were carried out in three independent experiments in duplicate. The apparent K_m and V_{max} values

were calculated from the nonlinear regression analysis of experimental data according to the following Michaelis-Menten equation, and the results were graphically represented by Eadie-Hofstee plots. The kinetic constants were estimated by the software program Prism (Version 5.0.1, GraphPad, San Diego, CA) and were reported as the mean±standard deviation (SD) of the parameter estimate.

In Vitro Biosynthesis and Isolation of Major Metabolite

The predominant metabolite 8-hydroxy-gomisin A was biosynthesized using human liver microsomes. The incubation system was scaled up to 250 mL. GA (500 μM) was incubated with the liver microsomes (final protein concentration, 1.0 mg/mL) and the NADPH-generating system (1 mM NADP+, 10 mM glucose-6-phosphate, 1 unit/mL of glucose-6-phosphate dehydrogenase, and 4 mM $MgCl_2$) for 4 h at 37°C. Under these conditions, approximately 10% of GA was converted to 8-hydroxy-gomisin A. Methanol (250 mL) was added to the reaction mixture to precipitate the protein. After centrifuging at 20,000×*g* for 20 min at 4°C, the supernatant was separated and extracted with ethyl acetate (250 mL×3). The organic layer was combined and dried in vacuo, the residue was re-dissolved in methanol (1.5 mL), and the solution was injected into the LC column. The HPLC system (SHIMADZU, Kyoto, Japan) consisted of a SCL–10A system controller, two LC–10AT pumps, a SIL–10A auto injector, a SPD–10AVP UV detector, and a C18 column (4.6 mm×150 mm, 10 μm) and was used to separate GA and its metabolite. The mobile phase was 55% methanol in water. The eluent was monitored at 254 nm with a flow rate of 1.0 mL/min, and the fractions containing 8-hydroxy-gomisin A were collected and dried in vacuo. The purity of 8-hydroxy-gomisin A was approximately 98% by HPLC-UV analysis.

Nuclear Magnetic Resonance Spectrometry

Nuclear magnetic resonance (NMR) spectra were measured with a 400 MHz Bruker spectrometer using tetramethylsilane as the reference for ^1H NMR. The compounds were dissolved in DMSO-d6, and the experiments were conducted at 23°C. Chemical shifts are reported in parts per million (ppm).

Docking Simulations

Docking simulation was performed using the knowledge-based homology modeling package from Advanced Protein Modeling (APM) that was distributed within SYBYL (X-1.1). The homology model of CYP3A5 was constructed based on the template structure of CYP3A4 (PDB ID: 3TJS). The sequences of both 3A4 (UnitProt ID: 08684) and 3A5 (UnitProt ID: 20815) were obtained from the PubMed protein sequence database. After backbone and variable modeling, a 1000-step minimization was carried out to obtain a low-energy conformation without any steric clashes between side chains. The model of CYP3A5 was analyzed and evaluated using the ProTable module and showed a high Ramachandran graph score of 98.2% (Supplemental Fig. S2). With the established 3D structure of 3A5 as well as the crystal structure of 3A4, the bioactive binding conformations of GA were generated using Surflex-Dock and were evaluated by an empirical function ChemScore, one of the most suitable scoring functions for P450s. The binding conformations of CYP3A4 (PDB ID: 3TJS) with bufalin, nifedipine, midazolam, and deoxyschizandrin were generated using Surflex-Dock. The docking results were further visualized using PyMOL Molecular Graphics System, version 0.99 (DeLano Scientific LLC). A 2D molecular descriptor (Discovery Studio Visualizer software, version 3.5) was employed to show the interacting amino acid residue plot of ligands located within the CYP3A4 active site.

Comparative Evaluation of Inhibitory Activities

To detect the selective inhibitory activities of GA towards CYP3A4 and CYP3A5, the effects of GA on CYP3A-catalyzed midazolam 1′-hydroxylation, nifedipine dehydrogenation, testosterone 6β-hydroxylation, and deoxyschizandrin 7-hydroxylation were determined using rhCYP3A4/5 and individual-donor human liver microsomes with different proportions of CYP3A4/5 proteins. The substrates were used at concentrations approximately equal to their respective K_m values as follows: 10 μM MDZ, 20 μM NIF, 50 μM TST, and 5 μM DS. All of the substrates and GA were previously dissolved in methanol, and the final methanol concentrations in the reaction mixtures did not exceed 1% (*v*/*v*). The substrates were incubated with 0.2 mg protein/ml HLMs or 20 nM rhCYP3A4/5 in the absence and presence of GA (concentration ranged from 0.1 to 100 μM). After 3 min of incubation at 37°C, the reaction was initiated by adding an NADPH-generating system, and further incubation followed for 10 min at 37°C in a shaking water bath. The reaction was terminated by the addition of 200 μl of methanol. The mixture was kept on ice until it was centrifuged at 20,000*g* for 20 min at 4°C. Aliquots of the supernatant were then taken for further UFLC analyses. All of the incubations throughout this study were conducted in triplicate.

Detecting Inducer-Mediated Alteration of CYP3A4 Activity in Living Cells

Cell Culture

HepG2 (1×10^6/well) cell lines were cultured in complete DMEM containing 10% FCS as a monolayer in a 96-well plate and were treated for 72 h with various concentrations of GA (1–300 μM). The final concentration of DMSO did not exceed 0.1% (*v*/*v*) in the culture media. Seventy-two hours after treatment, the effects of GA against the viability of treated cells were assessed using a CCK-8 assay kit (Solarbio, Beijing, China). Then, a cell-based assay was used to study the CYP3A4 catalytic activity, where HepG2 cells (1×10^6/well) were cultured in 6-well plates for 2 days and treated for another 72 h with 10 μM of rifampin or with the 0.1% DMSO vehicle (control). Deoxyschizandrin was used as a control substrate; deoxyschizandrin was metabolized by both CYP3A4 and CYP3A5 [17]. Two milliliters of incubation medium containing 20 μM of GA or 20 μM of deoxyschizandrin was added concomitantly to each well and incubated for 60 min at 37°C. The medium was collected and stored at −20°C until analysis. The cells were lysed with RIPA

buffer (50 mM Tris–HCl, pH 7.4, 150 mM NaCl, 1.0 mM EDTA, 0.1% SDS, 1.0% Triton X-100, 1.0% sodium deoxycholate), and the protein concentration in each well was quantified according to the manufacture's protocol using a Lowry protein assay kit (Mbchem, Shanghai, China).

Quantitative Real-Time PCR Analysis

Total RNA was isolated from cell pellets using the *RNAiso Plus* reagent with gDNA Eraser (Takara) according to the manufacturer's protocol. The yield and purity were measured by the ratio of A260/A280 using an ultraviolet spectrophotometer. A portion of 500 ng of RNA was subjected to reverse transcription in a 20-μL reaction mixture using a *PrimeScript*™ RT reagent Kit (Takara). After the synthesis of cDNA, real-time PCR was conducted with a SYBR® *Premix Ex Taq*™ II Kit (Takara) to detect the transcript levels of CYP3A4 and CYP3A5. The primer sequences for real-time PCR are listed in supplemental Table S1. The data were analyzed with Applied Biosystems StepOne™ Real-Time PCR System software version 2.0 (Applied Biosystems). Each experiment included standard curves for each cDNA and a no template control. The data were normalized to GAPDH.

Statistical Analysis

All statistical analyses were done by program Prism (Version 5.0.1, GraphPad, San Diego, CA). $P<0.05$ were considered as significant in the two-tailed Student's *t* test.

RESULTS

Identification of GA Metabolites

First, to identify the metabolites of GA, *in vitro* incubation studies were performed. Two new chromatographic peaks were specifically observed in human liver microsomes (HLM) after incubation with GA in the NADPH-generating system. The formation of these two metabolites was NADPH- and microsome-dependent (Supplemental Fig. S3). The $[M+K]^+$ ion of M2 at *m/z* 471 implied that M2 was a monoxide of the substrate (Supplemental Fig. S4 and Table S2). Moreover, the $[M+K]^+$ ion of M1 at *m/z* 443 implied that M1 was demethylene-gomisin A (DGA) (Supplemental Fig. S4 and Table S2). The primary metabolite (M2) was biosynthesized and fully identified as 8-hydroxy-gomisin A (8-HGA, Fig. 1) based on ^{1}H nuclear magnetic resonance (NMR) analyses (Supplemental Table S3). The most distinctive spectra changes were involved in the C-8 region between GA and M2. The multiplet of the C-8 proton signal at 1.66 ppm (1H, m) in GA was replaced by the singlet and shifted downfield to 3.61 ppm (1H, s) in the metabolite M2. Moreover, the C-8-methyl proton signal of M2 showed a downfield shift of 0.91 ppm compared with GA. These observations strongly suggested that hydroxylation occurred at the C-8 site. Furthermore, no conjugates were observed in the UDP-glucuronic acid (UDPGA)-, 3′-phosphoadenosine-5′-phosphosulfate (PAPS)-, and *S*-adenosyl-L-methionine (SAM)-generating systems when GA was incubated with either HLM or S9 fractions (data not shown).

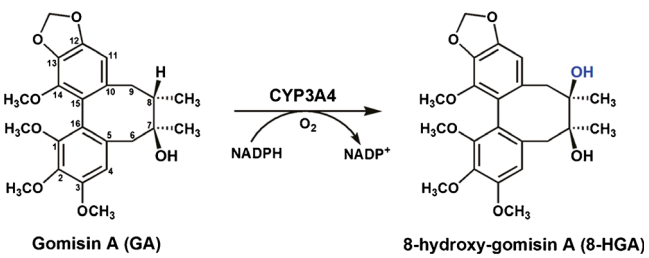

Fig. 1. The structure of GA and CYP3A4-catalyzed GA hydroxylation

Assays with Recombinant Human CYP Isoforms

To elucidate P450 isoforms involved in the metabolism of GA in humans, the activity of GA hydroxylation was determined in 14 rhCYP isoforms. Interestingly, GA 8-hydroxylation was predominantly catalyzed by CYP3A4 but was only limitedly catalyzed by CYP3A5 at different substrate concentrations tested (5 and 50 μM) (Fig. 2). However, regarding DGA formation, multiple isozymes, including CYP1A1, CYP2C9, CYP2C19, CYP2D6, CYP3A4, and CYP3A5, were involved (Supplemental Fig. S5).

Chemical Inhibition Assays

The inhibitory effects of selective chemical inhibitors of various CYPs on GA hydroxylation were investigated in pooled HLM incubations (Fig. 3). ABT, a broad P450 inactivator, inhibited GA hydroxylation completely, suggesting that P450s were the enzymes responsible for GA hydroxylation. Among the 11 selective inhibitors tested, ketoconazole (a potent inhibitor of CYP3A) and CYP3cide (a potent and selective inhibitor of CYP3A4) inhibited GA 8-hydroxylation by 100% ($P<0.05$). In contrast, other CYP inhibitors exhibited negligible inhibitory effects on GA hydroxylation. These results demonstrated that GA 8-hydroxylation was selectively catalyzed by CYP3A4 in humans.

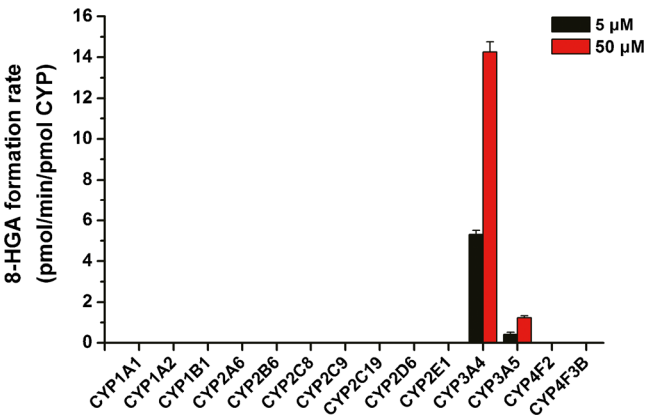

Fig. 2. Isozymes involved in the GA 8-hydroxylation reaction. Data represent the mean±SD from three experiments carried out in duplicate

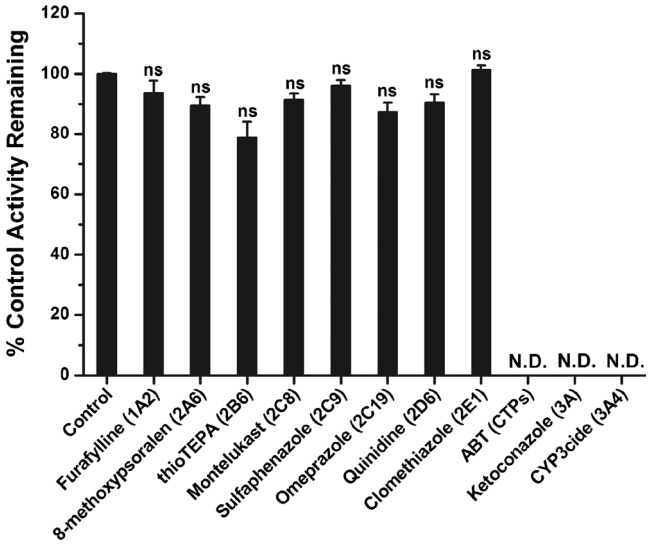

Fig. 3. Effects of selective P450 inhibitors on GA 8-hydroxylation in pooled HLM. Results are the mean±SD from three experiments carried out in duplicate. *N.D.* not determined. *ns*: $P>0.05$

Correlation Study

For GA hydroxylation to 8-HGA, strong correlations were observed with the content of CYP3A4 (Supplemental Table S4) ($r=0.950$, $P<0.0001$) as well as the activity of CYP3A4 ($r=0.891$, $P<0.0001$) in a panel of 13 individual HLMs (Fig. 4a, b). In contrast, as shown in Fig. 4c, d, very poor correlations were obtained for the formation rate of 8-HGA with the content of CYP3A5 ($r=0.381$, $P=0.199$) and the activity of CYP3A5 ($r=0.167$, $P=0.589$). The correlation study, together with reaction phenotyping assays and chemical inhibition assays, confirmed the predominant role of CYP3A4 in GA 8-hydroxylation.

Kinetic Analysis

To characterize the isoform-specific biotransformation mediated by CYP3A4, comparative kinetic evaluations were performed with rhCYP3A4 and rhCYP3A5. Based on the indication of linear Eadie–Hofstee plots, GA 8-hydroxylation in rhCYP3A4 followed Michaelis–Menten kinetics (Fig. 5a). Moreover, GA 8-hydroxylation in HLMs displayed similar K_m values as in rhCYP3A4 (Table I and Fig. 5b), indicating

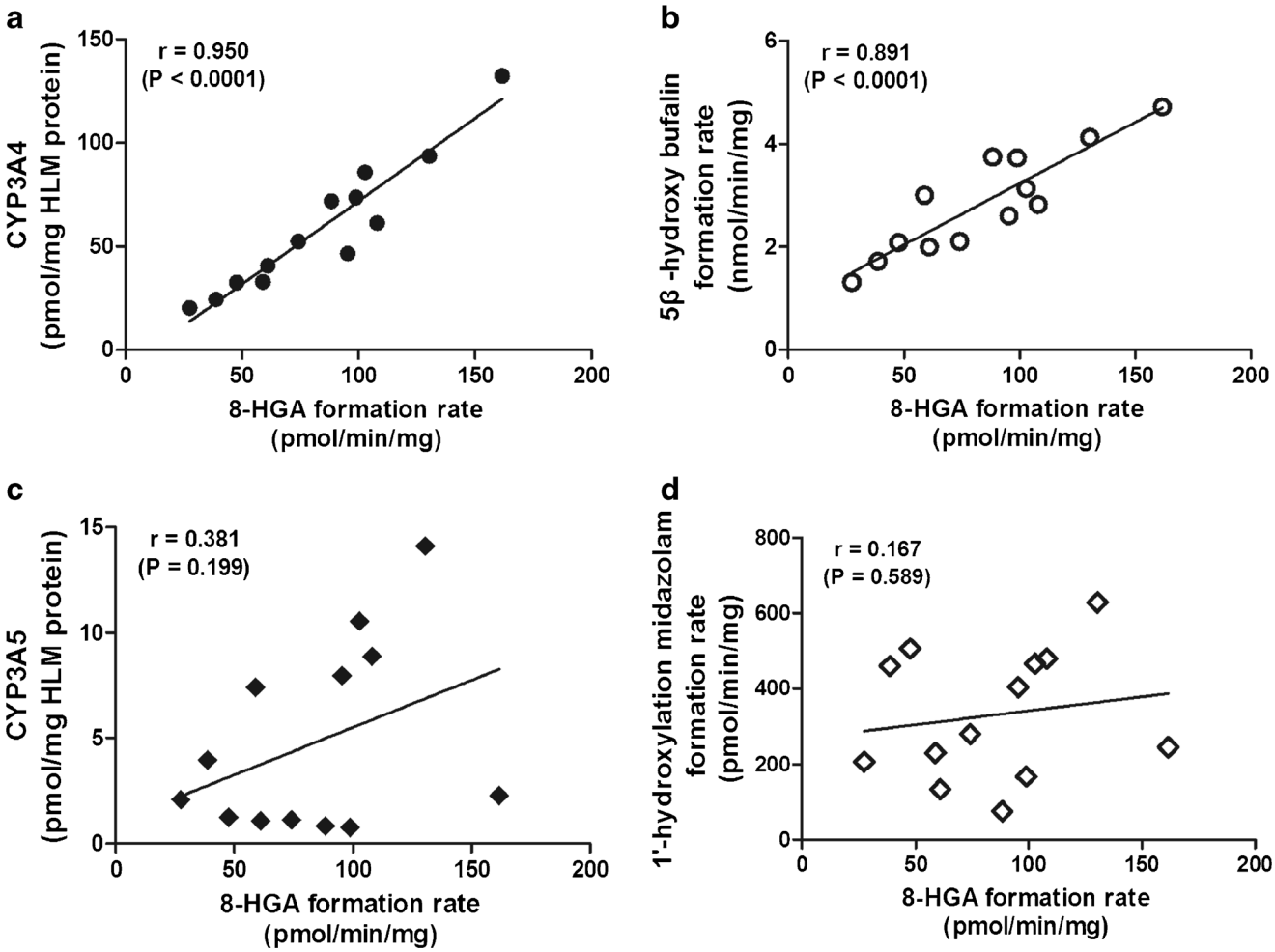

Fig. 4. Correlation studies between the formation rate of 8-HGA and the level of CYP3A4 content (**a**), CYP3A4 activity determined by bufalin 5β-hydroxylation (**b**), level of CYP3A5 content (**c**), and CYP3A5 activity determined by midazolam 1′-hydroxylation (**d**), in a panel of thirteen HLMs from individuals

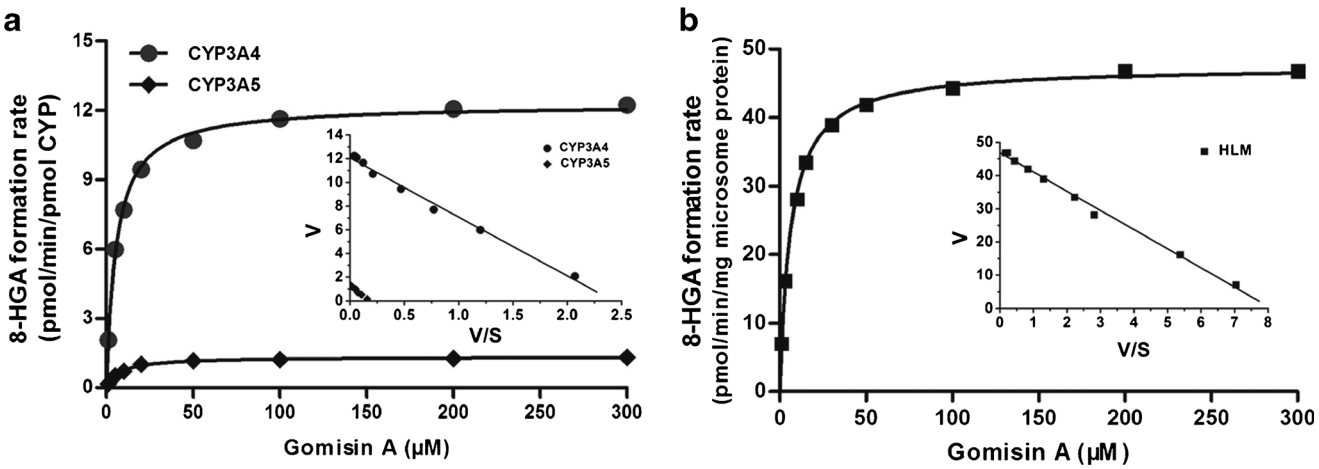

Fig. 5. Michaelis–menten kinetic plots of GA 8-hydroxylation catalyzed by rhCYP3A4, rhCYP3A5 (**a**) and pooled human liver microsomes (**b**). Eadie-Hofstee plots were inserted. Results are the mean±SD from three experiments carried out in duplicate

that CYP3A4 was the major enzyme participating in GA 8-hydroxylation. Although the K_m value of GA in rhCYP3A4 was not much lower than that in rhCYP3A5 (5.6±0.32 μM *vs.* 7.8±0.51 μM), the V_{max} values of GA 8-hydroxylation catalyzed by CYP3A5 was much lower than that by CYP3A4 (1.3±0.02 pmol/min/pmol CYP *vs.* 12.3±0.13 pmol/min/pmol CYP). Consequently, there was a 12.8-fold difference on intrinsic clearance (CL_{int}) between CYP3A4- and CYP3A5-mediated GA 8-hydroxylation (Table I). These results suggested that GA could serve as a highly selective probe for the evaluation of CYP3A4 activity in biological samples. Based on the above results, the proposed probe reaction of CYP3A4-catalyzed GA hydroxylation is shown in Fig. 1.

Inhibitory Effects of GA Against CYP3A4 and CYP3A5

The inhibitory activities of GA towards CYP3A4 and CYP3A5 were compared using rhCYP3A4/5 and individual-donor human liver microsomes with different proportions of CYP3A4/5 proteins, respectively. With a decrease in the CYP3A5 proportion from HLM-7 to HLM-8 (Supplemental Table S4), the inhibitory potentials (IC_{50}s) of GA towards the metabolism of CYP3A4/5 substrates increased and the IC_{50}s shifted to the left (Fig. 6a–d). The IC_{50} value for midazolam, nifedipine, testosterone, and deoxyschizandrin in HLM-7 (high CYP3A5 content) was 12-fold, 2.0-fold, 2.0-fold, and 4.1-fold higher than that in HLM-8 (low CYP3A5 content) (Table II). Similarly, the inhibitory potentials of GA towards these four CYP3A4/5 substrates increased in rhCYP3A4 compared with those in rhCYP3A5 and the IC_{50}s shifted to the left (Fig. 6e–h). The IC_{50} value of GA towards midazolam, nifedipine, testosterone, and deoxyschizandrin in rhCYP3A5 was 5-fold, 3.1-fold, 2.4-fold, and 5.6-fold higher than those in rhCYP3A4 (Table II). These findings demonstrated that GA can more strongly inhibit the activity of CYP3A4 than CYP3A5, which further indicated that GA showed a higher metabolic selectivity to CYP3A4 than to CYP3A5.

Table I. Kinetic Parameters of GA 8-Hydroxylation Catalyzed by Pooled HLM As Well As rhCYP3A4 and rhCYP3A5

Enzyme source	V_{max}	K_m	CL_{int}
Pooled HLM	47.5±0.4	6.3±0.3	7.54
rhCYP3A4	12.3±0.1	5.6±0.3	2.20
rhCYP3A5	1.30±0.02	7.8±0.5	0.17
Ratio (3A4/3A5)	9.5		12.8

K_m values are in μM; V_{max} values are in pmol/min per milligram for liver microsomes or in pmol/min per pmol P450 for CYP3A4 and CYP3A5. Intrinsic clearance (CL_{int}) is obtained by V_{max}/K_m and is in μl/min per milligram for liver microsomes or in μl/min per pmol P450 for CYP3A4 and CYP3A5. Data are shown as the mean±SD of three determinations performed in duplicate

Docking Simulations

Molecular docking studies were conducted to explore the difference in GA 8-hydroxylation between CYP3A4 and CYP3A5. As shown in Fig. 7a, b, the bioactive pose of GA in 3A4 was given a higher ChemScore value than that in 3A5 (−25.4528 *vs.* −21.2021). In addition, the distance between the H atom of the C-8 site and the heme of CYP3A4 (4.96 Å) was shorter than that of CYP3A5 (7.21 Å). In the conformation of CYP3A4, H-bonding between the oxygen atom of C3-methoxyl and Leu-483 was prominent and a π–π interaction between the benzene ring of GA and Phe-304 was also observed; this interaction stabilized the conformation (Fig. 7c). Only H-bonding between the oxygen atom of C1-methoxyl and Arg-105 was observed in the conformation of CYP3A5 (Fig. 7d). The docking results suggested that CYP3A4 may confer a more metabolically favorable state for GA than CYP3A5 and provided a structural explanation for the metabolic selectivity of GA for CYP3A4.

Monitoring the Modulation of CYP3A4 Activity in Living Cells by GA

Furthermore, GA was used to detect CYP3A4 activity to represent its gene induction by rifampin, a well-known CYP3A4 inducer, in HepG2 cell lines. The gene expression of CYP3A4 and CYP3A5 was analyzed by real-time RT-PCR. Compared with the control group, the CYP3A4 mRNA level was significantly upregulated by 2.4-fold in the rifampin-treated

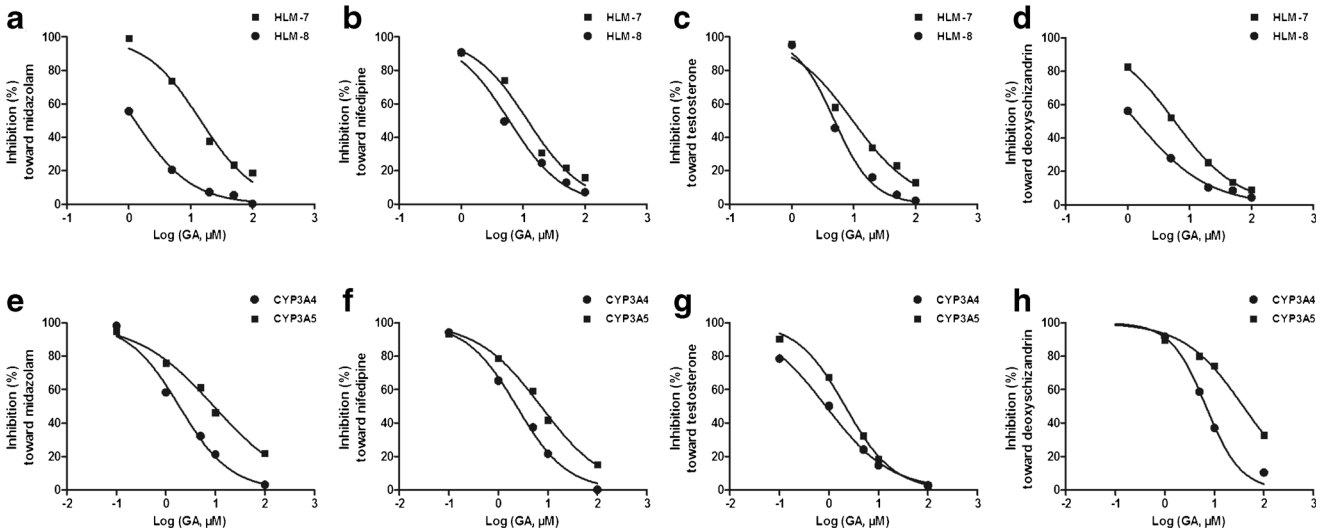

Fig. 6. The selective inhibitory effects of GA on CYP3A4/5 co-substrates in individual-donor HLMs with different proportions of CYP3A4 and CYP3A5 proteins (**a**–**d**), as well as in rhCYP3A4 and rhCYP3A5 systems (**e**–**h**). Data are shown as mean±SD from three experiments carried out in duplicate

group (Fig. 8a). The mRNA expression level of CYP3A5 was not markedly induced by rifampin (Fig. 8a). GA was low toxic to HepG2 cells, and its IC_{50} value in cell survival was as high as 61.5 μM (Supplemental Fig. S6). This concentration was almost 12 times greater the K_m value of GA 8-hydroxylation catalyzed by CYP3A4. The GA 8-hydroxylation formation rates in the medium after 60 min incubations were increased by 2.3-fold (Fig. 8b), which is consistent with the mRNA expression level of CYP3A4. In contrast, the hydroxylated metabolite formation rate of deoxyschizandrin, a co-substrate for CYP3A4 and CYP3A5, showed no significant difference between the control group and the rifampin-treated group (Fig. 8b). These results suggested that the induced expression of CYP3A4 gene could be selectively probed by a GA 8-hydroxylation assay.

DISCUSSION

CYP3A4 and CYP3A5 exhibit significant overlap in substrate specificity but can behave differently with regard to catalytic activity and inhibition potency. Therefore, an isoform-specific CYP3A4 probe would greatly help identify the differentiated activity between the two CYP3A isoforms and attenuate the variation of drug response. In the present study, we identify the novel selective probe reaction of GA hydroxylation to human CYP3A4. The hydroxylation of GA is selectively catalyzed by CYP3A4. The metabolite of GA was isolated and identified as 8-hydroxylation GA by LC-MS and ^{1}H-NMR. The CYP3A4-specific probe reaction of GA 8-hydroxylation followed ideal Michaelis–Menten kinetics and was well characterized by assays using recombinant P450s as well as chemical inhibition and correlation studies.

GA has distinct advantages in terms of isoform selectivity. Compared to quinidine, a reportedly selective CYP3A4 probe [30], GA exhibited a higher ratio (9.5-fold) of catalytic velocity for CYP3A4 and CYP3A5 (Table I and Fig. 5a), while this ratio is only about 4-fold for quinidine [31], and the non-ignorable contribution of CYP3A5 for quinidine 3-hydroxylation has also been reported [32]. In spite of a higher transformation efficiency (V_{max}) of quinidine, the intrinsic clearance (CL_{int}) is offset due to its much lower affinity (high K_m value) to CYP3A4 [33] as compared to GA. Similarly, the dominant contribution of CYP3A4 to GA 8-hydroxylation was characterized by a higher CL_{int} ratio (12.8-fold) for CYP3A4 and CYP3A5 than that of other CYP3A4-preferred substrates, e.g., simvastatin, diltiazem, and verapamil [34]. These suggested that GA was more selective to CYP3A4 than other CYP3A4 substrates.

With respect to the structure of ligands, it is worth noting that the dibenzocyclooctadiene lignans with six methoxy groups on two benzene rings is the most potent co-substrate

Table II. Selective Inhibitory Effects of GA on CYP3A Substrates in Two Individual-Donor HLMs with Different Proportions of CYP3A4 and CYP3A5 Proteins As Well As in rhCYP3A4 and rhCYP3A5

		IC_{50} (HLMs)			IC_{50} (rhCYPs)		
Substrates	Reaction	HLM-7[a]	HLM-8[a]	Ratio (HLM-7/HLM-8)	rhCYP3A5	rhCYP3A4	Ratio (3A4/3A5)
Midazolam	1′-Hydroxylation	14.5	1.26	12	9.26	1.86	5.0
Nifedipine	Dehydrogenation	11.9	5.96	2.0	7.22	2.34	3.1
Testosterone	6β-Hydroxylation	9.65	4.89	2.0	2.12	0.87	2.4
Deoxyschizandrin	7-Hydroxylation	5.71	1.39	4.1	38.0	6.74	5.6

IC_{50} values are in μM

[a] The total amounts of CYP3A4 and CYP3A5 protein from the no. 7 and no. 8 individual-donor human liver microsomes (HLM-7 and HLM-8) are approximately equal, while the CYP3A5 amount in HLM-7 is almost 12-fold higher than that in HLM-8 (as shown in Supplemental Table S4).

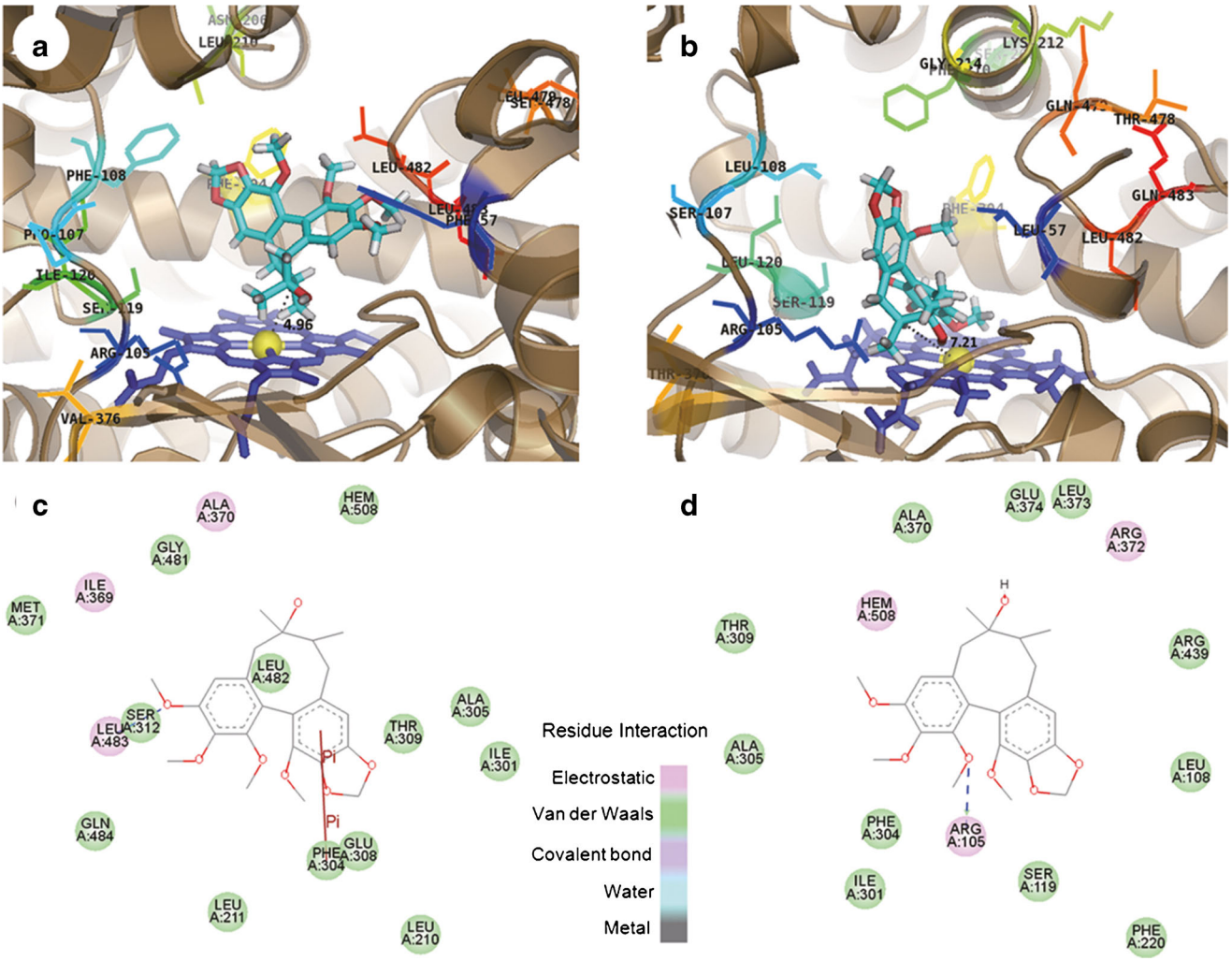

Fig. 7. Docking simulation of GA into CYP3A4 (**a**) and CYP3A5 (**b**). The interacting amino acid residues plot of GA located within the active site of CYP3A4 (**c**) and CYP3A5 (**d**). Heme and iron atoms are coloured in *blue violet* and *yellow*, respectively

of CYP3A4 and CYP3A5, such as deoxyschizandrin 7-hydroxylation [17]. In contrast, the lignans preferred to be selectively metabolized by CYP3A4, but not CYP3A5, in cases when the C-7 of the lignans was hydroxylated, such as GA 8-hydroxylation and schizandrin 8-hydroxylation [18]. However, 8-hydroxylation schizandrin undergoes subsequent rapid demethylation by CYP3A4, which might affect the accurate quantification of the total intrinsic metabolic clearance of CYP3A4.

More interestingly, the substrates appeared to be selectively metabolized by CYP3A4 through hydroxylation reactions, such as GA 8-hydroxylation, schizandrin 8-hydroxylation [18], bufalin 5β-hydroxylation [14], and resibufogenin 5β-hydroxylation [35]. In contrast, the dealkylation reactions of substrates are generally mediated by multiple CYP enzymes other than CYP3A4. The minor reaction of GA demethylene is primarily catalyzed by CYP1A2 and, to a lesser extent, by CYP3A4 (Supplemental Fig. S5). Similarly, CYP1A2 and CYP3A4 are jointly involved in the N-dealkylation of propafenone [36] and O-demethylation of verapamil [37]. These findings hinted that CYP3A4-specific probes might favor the hydroxylation reaction of compounds with a rigid polycyclic skeleton.

As for the structure of enzymes, we noted that the amino acid residues Phe57, Pro107, Phe108, Asn206, Leu210, Arg212, Asp214, Val376, Ser478, and Leu479 within the substrate recognition sites of CYP3A4 differed from those of CYP3A5 (Leu57, Ser107, Leu108, Ser206, Phe210, Lys212, Gly214, Thr376, Asp478, and Thr479) [38, 39]. Among these, Asp214 and Leu479 are involved in the active site of CYP3A4 [40, 41]. On one hand, acidic Asp214in CYP3A4 was replaced by neutral Gly214 in CYP3A5, while hydrophobic Leu479 in CYP3A4 was replaced by polar Thr479 in CYP3A5. These replacements might change the electrostatic and hydrophobic interaction between enzymes and substrates. On the other hand, Phe57, Pro107, Phe108, Asn206, Arg212, Asp214, and Leu479 within CYP3A4 are substituted by smaller Leu57, Ser107, Leu108, Ser206, Lys212, Gly214, and Thr479 within CYP3A5. These substitutions might change the conformational matching between enzymes and substrates [42], resulting in the better adaptability of CYP3A4 to GA (a rigid molecule) or making GA fail to orient itself in

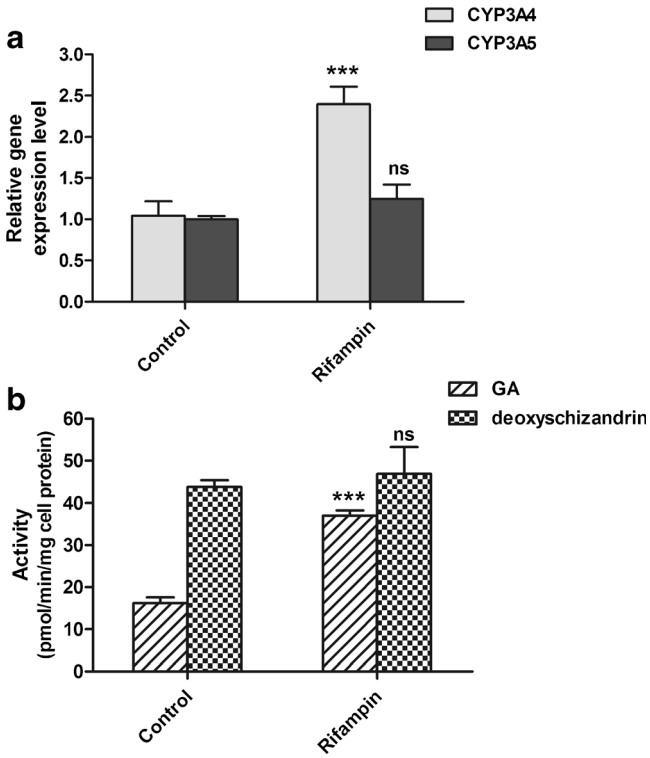

Fig. 8. **a** Relative gene expression levels ($2^{-\triangle\triangle CT}$) of CYP3A4 and CYP3A5 normalized to GAPDH in hepG2 cells after treatment of 10 μM rifampin for 72 h. Each value represent the mean±SD (n=6). **b** Detection of rifampicin-induced CYP3A4 expression in a hepG2 cell-based assay using GA as a probe and deoxyschizandrin as a control substrate. Data are shown as mean±SD from three experiments carried out in duplicate. ***P<0.001; ns: P>0.05

the CYP3A5 active site. A total of 20 poses were obtained for the docking of GA in the active site of CYP3A4. The optimal binding mode was identified. In this conformation, a hydrogen bonding interaction between the oxygen atom of C3-methoxyl and Leu-483 was noted, along with a hydrophobic π–π interaction between the benzene ring and Phe-304; a residue lies on the I helix that has a key role in regioselectivity and stereoselectivity [41, 43]. Therefore, these findings could, in part, explain why the catalytic activity of CYP3A4 for GA 8-hydroxylation was much higher than that of CYP3A5.

Generally, a probe substrate can act as both a substrate and an inhibitor of the same enzyme. Different inhibitory activities of GA towards CYP3A4 and CYP3A5 were noted. In liver microsomes from two individual donors, the CYP3A4 protein contents were almost equal, but the CYP3A5 level was comparable. The inhibitory potentials of GA increased with the decrease of the CYP3A5 protein levels for the four typical co-substrates of CYP3A4/5: midazolam, nifedipine, testosterone, and deoxyschizandrin [17]. Specifically, when the contribution of CYP3A5 increased for the substrate metabolism, the inhibitory efficiency of GA decreased and vice versa. Likewise, in the recombinant P450s systems, the inhibitory activities of GA towards CYP3A4-catalyzed metabolism were higher than that towards CYP3A5-catalyzed metabolism. These findings further suggested that GA exhibited a higher metabolic selectivity to the CYP3A4 enzyme.

In addition to the selective phenotyping of CYP3A4 in microsomes, it is necessary to distinguishably detect the CYP3A4 activity in living cells for a gene induction assay. Thus, in the present study, GA was also used to detect CYP3A4 activity to represent its gene induction by rifampin, a well-known CYP3A4 inducer, in HepG2 cell lines. GA was relatively nontoxic to HepG2 cells, even at a high substrate concentration (near 10 K_m value), consistent with findings that were previously reported [21]. However, bufalin, another reportedly CYP3A4-specific probe [14], showed strong cytotoxic effects on HepG2 cells, with IC_{50} values in the range of 0.12 to 0.81 μM [19, 44], far lower than its K_m value (10 μM) [14]. Because of toxicity, the application of bufalin in measuring CYP3A4 activity in living cells is limited. Additionally, GA exhibits high membrane permeability with a passive diffusion manner [45], which provides the possibility of performing a cell-based assay. The CYP3A4 mRNA level was significantly upregulated in the rifampin-treated group, while the CYP3A5 mRNA level was not remarkably induced, possibly because CYP3A5 is far less susceptible to induction than CYP3A4 [46]. In spite of the low-amplitude increase of the CYP3A4 mRNA level in hepG2 cells treated by rifampin, GA successfully probes the CYP3A4 activity, consistent with its mRNA expression level. However, deoxyschizandrin cannot selectively detect the change in CYP3A4 activity caused by rifampin, at least partly because of the non-negligible contribution of CYP3A5 to its metabolism, even though the catalytic rate of CYP3A towards deoxyschizandrin was almost 3 times faster than towards GA (Fig. 8b). These results suggested that the induction of the human gene expression of CYP3A4 could be selectively probed by a GA 8-hydroxylation assay. Furthermore, the possibility of GA serving as an *in vivo* probe for clinical DDI risk assessment could not be ruled out due to its high isoform selectivity and excellent safety potential. However, further preclinical pharmacokinetics and *in vivo* sensitivity to inhibition/induction of GA should be thoroughly investigated before it enters clinical trials.

CONCLUSION

In summary, GA 8-hydroxylation was a probe reaction that was highly selective for human CYP3A4. This probe followed ideal Michaelis–Menten kinetics, with a relatively high affinity. The differential ligand–residue interactions determined the catalytic selectivity of GA 8-hydroxylation between CYP3A4 and CYP3A5. GA was not toxic to living cells at concentrations near its K_m value. GA has been successfully applied for the real-time monitoring of the modulation of CYP3A4 activities by inducers. These results strongly suggested that GA with a dibenzocyclooctadiene skeleton can be used as a novel probe to represent the catalytic function of CYP3A4 in various biological samples, such as liver microsomes and living cells.

ACKNOWLEDGMENTS

This present study was financially supported by grants from the National Natural Science Foundation of China

(81403003, 81573501, and 81402985) and the National Key Technology Major Project of China (2012ZX09506001, 2012ZX10002011, and 2012ZX09501001).

Authorship Contributions Participated in research design: Wu, Ge, He, and Yang. Conducted experiments: Wu, Wang, Dai, Ning, and Hu. Performed data analysis: Wu, Ge, He, Wang, and Yang. Wrote or contributed to the writing of the manuscript: Wu, Ge, He, and Yang.

REFERENCES

1. Thummel KE, Wilkinson GR. In vitro and in vivo drug interactions involving human CYP3A. Annu Rev Pharmacol. 1998;38:389–430.
2. Paine MF, Khalighi M, Fisher JM, Shen DD, Kunze KL, Marsh CL, *et al.* Characterization of interintestinal and intraintestinal variations in human CYP3A-dependent metabolism. J Pharmacol Exp Ther. 1997;283(3):1552–62.
3. Kuehl P, Zhang J, Lin Y, Lamba J, Assem M, Schuetz J, *et al.* Sequence diversity in CYP3A promoters and characterization of the genetic basis of polymorphic CYP3A5 expression. Nat Genet. 2001;27(4):383–91.
4. Aoyama T, Yamano S, Waxman DJ, Lapenson DP, Meyer UA, Fischer V, *et al.* Cytochrome-P-450 Hpcn3, a novel cytochrome-P-450 Iiia-gene product that is differentially expressed in adult human-liver - Cdna and deduced amino-acid sequence and distinct specificities of Cdna-expressed Hpcn1 and Hpcn3 for the metabolism of steroid-hormones and cyclosporineu. J Biol Chem. 1989;264(18):10388–95.
5. Huang WL, Lin YS, McConn DJ, Calamia JC, Totah RA, Isoherranen N, *et al.* Evidence of significant contribution from CYP3A5 to hepatic drug metabolism. Drug Metab Dispos. 2004;32(12):1434–45.
6. McConn DJ, Lin YS, Allen K, Kunze KL, Thummel KE. Differences in the inhibition of cytochromes P450 3A4 and 3A5 by metabolite-inhibitor complex-forming drugs. Drug Metab Dispos. 2004;32(10):1083–91.
7. Wang YH, Jones DR, Hall SD. Differential mechanism-based inhibition of CYP3A4 and CYP3A5 by verapamil. Drug Metab Dispos. 2005;33(5):664–71.
8. Eichelbaum M, Ingelman-Sundberg M, Evans WE. Pharmacogenomics and individualized drug therapy. Annu Rev Med. 2006;57:119–37.
9. Li AP. Screening for human ADME/Tox drug properties in drug discovery. Drug Discov Today. 2001;6(7):357–66.
10. Galetin A, Ito K, Hallifax D, Houston JB. CYP3A4 substrate selection and substitution in the prediction of potential drug-drug interactions. J Pharmacol Exp Ther. 2005;314(1):180–90.
11. Li AP. Evaluation of luciferin-isopropyl acetal as a CYP3A4 substrate for human hepatocytes: effects of organic solvents, cytochrome P450 (P450) inhibitors, and P450 inducers. Drug Metab Dispos. 2009;37(8):1598–603.
12. Patki KC, Von Moltke LL, Greenblatt DJ. In vitro metabolism of midazolam, triazolam, nifedipine, and testosterone by human liver microsomes and recombinant cytochromes p450: role of cyp3a4 and cyp3a5. Drug Metab Dispos. 2003;31(7):938–44.
13. Houston JB, Kenworthy KE. In vitro-in vivo scaling of CYP kinetic data not consistent with the classical Michaelis-Menten model. Drug Metab Dispos. 2000;28(3):246–54.
14. Ge GB, Ning J, Hu LH, Dai ZR, Hou J, Cao YF, *et al.* A highly selective probe for human cytochrome P450 3A4: isoform selectivity, kinetic characterization and its applications. Chem Commun. 2013;49(84):9779–81.
15. Ekroos M, Sjogren T. Structural basis for ligand promiscuity in cytochrome P450 3A4. Proc Natl Acad Sci U S A. 2006;103(37):13682–7.
16. Yano JK, Wester MR, Schoch GA, Griffin KJ, Stout CD, Johnson EF. The structure of human microsomal cytochrome P450 3A4 determined by X-ray crystallography to 2.05—a resolution. J Biol Chem. 2004;279(37):38091–4.
17. Wu J, Cao Y, Zhang Y, Liu Y, Hong JY, Zhu L, *et al.* Deoxyschizandrin, a naturally occurring lignan, is a specific probe substrate of human cytochrome P450 3A. Drug Metab Dispos. 2014;42(1):94–104.
18. Cao YF, Zhang YY, Li J, Ge GB, Hu D, Liu HX, *et al.* CYP3A catalyses schizandrin biotransformation in human, minipig and rat liver microsomes. Xenobiotica; the fate of foreign compounds in biological systems. 2010;40(1):38–47.
19. Qi FH, Inagaki Y, Gao B, Cui XY, Xu HL, Kokudo N, *et al.* Bufalin and cinobufagin induce apoptosis of human hepatocellular carcinoma cells via Fas- and mitochondria-mediated pathways. Cancer Sci. 2011;102(5):951–8.
20. Ye M, Han J, An DG, Tu GZ, Guo D. New cytotoxic bufadienolides from the biotransformation of resibufogenin by mucor polymorphosporus. Tetrahedron. 2005;61(37):8947–55.
21. Wan CK, Zhu GY, Shen XL, Chattopadhyay A, Dey S, Fong WF. Gomisin A alters substrate interaction and reverses P-glycoprotein-mediated multidrug resistance in HepG2-DR cells. Biochem Pharmacol. 2006;72(7):824–37.
22. Li D, Han YL, Meng XL, Sun XP, Yu Q, Li Y, *et al.* Effect of regular organic solvents on cytochrome P450-mediated metabolic activities in rat liver microsomes. Drug Metab Dispos. 2010;38(11):1922–5.
23. Bjornsson TD, Callaghan JT, Einolf HJ, Fischer V, Gan L, Grimm S, *et al.* The conduct of in vitro and in vivo drug-drug interaction studies: a PhRMA perspective. J Clin Pharmacol. 2003;43(5):443–69.
24. Walsky RL, Obach RS, Gaman EA, Gleeson JP, Proctor WR. Selective inhibition of human cytochrome P4502C8 by montelukast. Drug Metab Dispos. 2005;33(3):413–8.
25. Rae JM, Soukhova NV, Flockhart DA, Desta Z. Triethylenethiophosphoramide is a specific inhibitor of cytochrome P450 2B6: implications for cyclophosphamide metabolism. Drug Metab Dispos. 2002;30(5):525–30.
26. Emoto C, Murase S, Sawada Y, Jones BC, Iwasaki K. In vitro inhibitory effect of 1-aminobenzotriazole on drug oxidations catalyzed by human cytochrome P450 enzymes: a comparison with SKF-525A and ketoconazole. Drug Metab Pharmacokinet. 2003;18(5):287–95.
27. Walsky RL, Obach RS, Hyland R, Kang P, Zhou S, West M, *et al.* Selective mechanism-based inactivation of CYP3A4 by CYP3cide (PF-04981517) and its utility as an in vitro tool for delineating the relative roles of CYP3A4 versus CYP3A5 in the metabolism of drugs. Drug Metab Dispos. 2012;40(9):1686–97.
28. Liu XD, Hu LH, Ge GB, Yang B, Ning J, Sun SX, *et al.* Quantitative analysis of cytochrome P450 isoforms in human liver microsomes by the combination of proteomics and chemical probe-based assay. Proteomics. 2014;14(16):1943–51.
29. Niwa T, Murayama N, Emoto C, Yamazaki H. Comparison of kinetic parameters for drug oxidation rates and substrate inhibition potential mediated by cytochrome P450 3A4 and 3A5. Curr Drug Metab. 2008;9(1):20–33.
30. Nielsen TL, Rasmussen BB, Flinois JP, Beaune P, Brosen K. In vitro metabolism of quinidine: the (3S)-3-hydroxylation of quinidine is a specific marker reaction for cytochrome P-4503A4 activity in human liver microsomes. J Pharmacol Exp Ther. 1999;289(1):31–7.
31. Galetin A, Brown C, Hallifax D, Ito K, Houston JB. Utility of recombinant enzyme kinetics in prediction of human clearance: impact of variability, CYP3A5, and CYP2C19 on CYP3A4 probe substrates. Drug Metab Dispos. 2004;32(12):1411–20.
32. Allqvist A, Miura J, Bertilsson L, Mirghani RA. Inhibition of CYP3A4 and CYP3A5 catalyzed metabolism of alprazolam and quinine by ketoconazole as racemate and four different enantiomers. Eur J Clin Pharmacol. 2007;63(2):173–9.

33. Zhao XJ, Ishizaki T. The in vitro hepatic metabolism of quinine in mice, rats and dogs: comparison with human liver microsomes. J Pharmacol Exp Ther. 1997;283(3):1168–76.
34. Tseng E, Walsky RL, Luzietti RA, Harris JJ, Kosa RE, Goosen TC, *et al.* Relative contributions of cytochrome CYP3A4 versus CYP3A5 for CYP3A-cleared drugs assessed in vitro using a CYP3A4-selective inactivator (CYP3cide). Drug Metab Dispos. 2014;42(7):1163–73.
35. Ning J, Yu ZL, Hu LH, Wang C, Huo XK, Deng S, *et al.* Characterization of the phase I metabolism of resibufogenin and evaluation of the metabolic effects on its antitumor activity and toxicity. Drug Metab Dispos. 2015;43(3):299–308.
36. Botsch S, Gautier JC, Beaune P, Eichelbaum M, Kroemer HK. Identification and characterization of the cytochrome-P450 enzymes involved in N-dealkylation of propafenone - molecular-base for interaction potential and variable disposition of active metabolites. Mol Pharmacol. 1993;43(1):120–6.
37. Kroemer HK, Gautier JC, Beaune P, Henderson C, Wolf CR, Eichelbaum M. Identification of P450 enzymes involved in metabolism of verapamil in humans. N-S. Arch Pharmacol. 1993;348(3):332–7.
38. Lu Y, Hendrix CW, Bumpus NN. Cytochrome P450 3A5 plays a prominent role in the oxidative metabolism of the anti-human immunodeficiency virus drug maraviroc. Drug Metab Dispos. 2012;40(12):2221–30.
39. Wang H, Dick R, Yin H, Licad-Coles E, Kroetz DL, Szklarz G, *et al.* Structure-function relationships of human liver cytochromes P450 3A: aflatoxin B1 metabolism as a probe. Biochemistry. 1998;37(36):12536–45.
40. Szklarz GD, Halpert JR. Molecular modeling of cytochrome P450 3A4. J Comput Aided Mol Des. 1997;11(3):265–72.
41. Williams PA, Cosme J, Vinkovic DM, Ward A, Angove HC, Day PJ, *et al.* Crystal structures of human cytochrome P450 3A4 bound to metyrapone and progesterone. Science. 2004;305(5684):683–6.
42. Khan KK, He YQ, Domanski TL, Halpert JR. Midazolam oxidation by cytochrome P450 3A4 and active-site mutants: an evaluation of multiple binding sites and of the metabolic pathway that leads to enzyme inactivation. Mol Pharmacol. 2002;61(3):495–506.
43. Dong D, Wu B, Chow D, Hu M. Substrate selectivity of drug-metabolizing cytochrome P450s predicted from crystal structures and in silico modeling. Drug Metab Rev. 2012;44(2):192–208.
44. Miao Q, Bi LL, Li X, Miao S, Zhang J, Zhang S, *et al.* Anticancer effects of bufalin on human hepatocellular carcinoma HepG2 cells: roles of apoptosis and autophagy. Int J Mol Sci. 2013;14(1):1370–82.
45. Madgula VL, Avula B, Choi YW, Pullela SV, Khan IA, Walker LA, *et al.* Transport of schisandra chinensis extract and its biologically-active constituents across Caco-2 cell monolayers - an in-vitro model of intestinal transport. J Pharm Pharmacol. 2008;60(3):363–70.
46. Wrighton SA, Ring BJ, Watkins PB, Vandenbranden M. Identification of a polymorphically expressed member of the human cytochrome P-450iii family. Mol Pharmacol. 1989;36(1):97–105.